



# Morphological, electrical, dielectric, and complex electrical modulus studies of copper ion conducting HPMC/PVA hosted nanocomposite electrolyte films

N. Sandhya Rani<sup>1</sup> · H. D. Swapna<sup>2</sup> · R. Karthik<sup>1</sup> · C. Manasa<sup>3</sup>

Received: 2 August 2021 / Accepted: 4 December 2021 / Published online: 26 January 2022  
© The Author(s), under exclusive licence to Springer-Verlag GmbH Germany, part of Springer Nature 2021

## Abstract

Solution casting technique is tailored to synthesis the film samples of hydroxypropyl methylcellulose (HPMC)/poly vinylalcohol (PVA) blends embedded with various concentrations of copper oxide (CuO) nanoparticles (1–4%, wt%). The structural analysis by X-ray diffraction (XRD) confirmed the uniform dispersion of nano CuO into HPMC/PVA blends. The crystalline size as well as the percentage of crystallinity decreases with increasing concentration of CuO in all HPMC/PVA–CuO electrolyte systems. This reduced percentage of crystallinity greatly affects the conductivity property of the polymer electrolytes. The surface morphology and uniformity of phase formation of the samples were analyzed by scanning electron microscope (SEM). The samples were analyzed by using electrical impedance spectroscopy by LCR meter (ZM2376) with in the frequency range 50 Hz to 1 MHz. The dielectric constant decreases, while the AC electrical conductivity increases with increasing frequency. The plots of AC conductivity at high frequency region obey Jonscher Power Law. The frequency exponent (S) analysis for various temperature suggested that the correlated barrier hopping (CBH) model supports the ion transport mechanism at high temperatures for CuO (3 wt%) nanocomposite polymer electrolyte film. The presence of non-Debye type conductivity relaxation is observed in this reported polymer electrolytes by analyzing complex electrical modulus. The temperature dependent analysis of dielectric and AC conductivity properties increases with the increase in temperature. This may be due to the ion migration which is significantly improved by the addition of CuO nanoparticles. All estimated results of these nanocomposite polymer electrolytes are strongly convincing its use for the electrochemical cell device applications.

**Keywords** Polymer electrolyte · AC conductivity · Dielectric constant · Impedance · Complex electrical modulus

## Introduction

In recent years, polymer blends complexed with suitable nanoparticles are the specially focused materials for exhibiting unique chemical and physical properties and find wide applications in the fields of nano-electronic devices, super capacitors, etc. [1–3]. Electrolytes utilized in electronic

gadgets and batteries today might be high in conductivity, but they are unsafe and non-biodegradable. Hence, they are danger to the environment. In this regard, several researchers studied biodegradable polymer nanocomposites to improve the interfacial properties [4, 5].

The present work is focused on the preparation and data characterization of biodegradable polymer blends of hydroxypropyl methylcellulose (HPMC) and polyvinyl alcohol (PVA) incorporated with copper oxide (CuO) nanoparticles. HPMC polymer is more thermally stable when compared with cellulose derivatives like carboxymethylcellulose (CMC), hydroxyethylcellulose (HEC), and methylcellulose (MC) [6–8]. In our earlier work, we have reported that HPMC is capable of dissolving variety of metal salts

✉ N. Sandhya Rani  
sandhya.phy@vce.ac.in

<sup>1</sup> Department of Applied Physics, Vidyavardhaka College of Engineering, Mysuru 570-002, India

<sup>2</sup> Department of Physics, JSS College of Mysuru, Mysuru, India

<sup>3</sup> Department of Chemistry, Vidyavardhaka College of Engineering, Mysuru 570-002, India

and can form thin films with excellent stability [9, 10]. PVA is a water-dissolvable polymer with an excellent chemical resistance, thermal stability, and mechanical strength. As it is biodegradable and non-toxic, it is extensively used in textile, biomedical, and pharmaceutical industries [11, 12]. CuO is a low cost non-toxic p-type semiconductor material with excellent optical and electrical properties. It is extensively used in the preparation of optoelectronic and electronic gadgets like electrochemical cells, gas sensors, solar cells, and optical switches [13–15]. In view of its significance, many researchers are exploring its applications for various electrochemical device applications. Jundale et. al. (2013) reported structural and electrical transport properties of polyaniline-CuO hybrid nanocomposites. The results showed the electrical conductivity could be enhanced upon adding CuO nanoparticles into the polymer host [16]. Manjunath et. al. (2016) studied CuO:PVA nanocomposite electrolytes and reported that CuO nanoparticles doped PVA has greater ionic diffusivity and high ionic conductivity [4]. Alghunaim (2019) reported the effects of CuO nanofiller on spectroscopic and dielectric modulus properties of carboxymethyl cellulose (CMC) and polyvinyl pyrrolidone (PVP) polymer blend electrolytes. The results showed that the dielectric constant value reduced systematically with an increase in frequency which is ascribed to the presence of polarization effects [5]. Alhazime (2020) reported a study on the effects of nano CuO doping on the structural and thermal properties of PVA/PEG blends. The results showed that the CuO doped polymer blends got high thermal stability which could be due to the interaction occurred between the nano CuO and the hydroxyl groups of the polymer blends [17].

Though some research works have been reported on the charge carrier transport properties of doped polymers, no literature is available on HPMC/PVA-CuO nanocomposite polymer electrolyte films. Hence, incorporating CuO nanoparticles into the polymer blend matrix may bring remarkable structural and morphological changes, which results in the enhancement of their performance and properties such as conductivity, electrochemical stability, and sensitivity. Considering its significance, the current work is being started, and endeavors have been made to incorporate biodegradable polymer hosted nanocomposite electrolyte films (HPMC/PVA-CuO) that display great electrical conductivity.

## Experimental work

### Materials and synthesis of HPMC/PVA-CuO nanocomposites

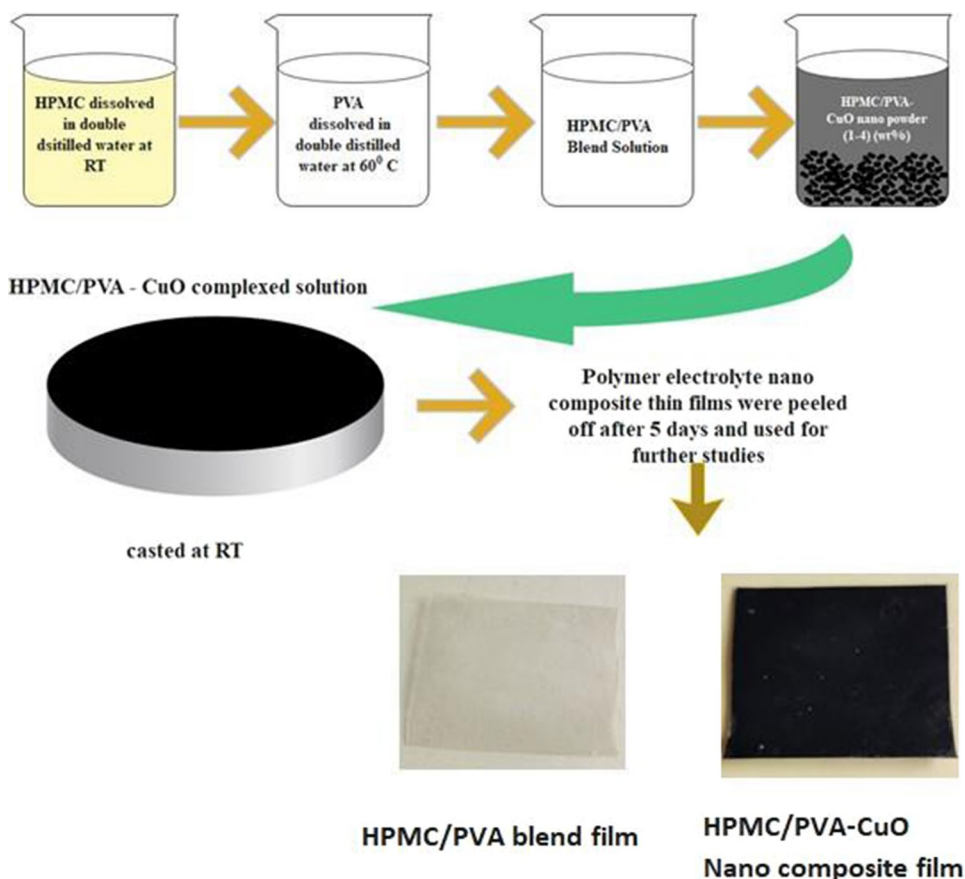
#### Sample preparation

Solution casting technique is adopted to prepare pure HPMC, pure PVA, and HPMC/PVA blends with different concentrations of CuO nanoparticles using double distilled water as solvent. PVA and HPMC-E15LV were purchased from Loba Chemicals India and were used without further purification. CuO nanoparticles were purchased from S. D. Fine Chemicals India. Here, 5% (wt%) of HPMC and PVA solutions were prepared separately. To prepare HPMC/PVA blends, the HPMC solution was added to that of PVA with constant stirring. The mixture of this solution was stirred overnight to obtain completely dissolved and clear solution. A 1–4% (wt%) of CuO nanoparticles was added slowly into the HPMC/PVA blend solution and stirred continuously for 2 h using magnetic stirrer at 380 rpm to ensure complete mixing. Then, the entire blend was degassed in a vacuum oven for 10 min and poured into the leveled glass plates to evaporate at room temperature for 5 to 6 days. The final obtained thin films were stored in desiccators to avoid moisture absorption. As the polymer samples complexed with 5% (wt%) CuO were very brittle and cracked, the higher added concentration of CuO is not suitable for thin film formation. Hence, the optimal complexing of CuO nanoparticles were carried out only up to 4% (wt%) and the HPMC/PVA-CuO nano-composite polymer electrolyte thin films (5:5:1, 5:5:2, 5:5:3, 5:5:4) with thickness varying from 0.12 to 0.24 mm were prepared successfully. Figure 1 displays compositions used in the preparation of HPMC/PVA-CuO nanocomposite polymer electrolyte films.

#### Instrumentation

The homogeneity of CuO nanoparticles into the HPMC/PVA polymer blend and also the crystallinity study of the prepared samples were done by using Rigaku Miniflex-II X-ray diffractometer with CuK $\alpha$  radiation ( $\lambda = 1.5406 \text{ \AA}$ ). The diffraction patterns were obtained for Bragg's angle ( $2\theta$ ) in the

**Fig. 1** Synthesis of HPMC/PVA-CuO nanocomposite polymer electrolyte films



scale of  $10^0 - 80^0$  with a scanning speed of  $5^0/\text{min}$  in the step size  $0.01^0$ . The scanning electron microscope (JEOL 840) with resolution at 20 kv is used to analyze the surface morphology of HPMC/PVA-CuO nanocomposite films. Before imaging, the reported samples were gold coated using the sputter coater at 10 mA current under 10–2 torr vacuum for 3 min. The dielectric and AC conductivity measurements of these samples were carried out for the frequencies ranging from 50 Hz to 1 MHz using LCR meter ZM2376. The disk shape sample (13 mm in diameter) was placed in between the stainless steel electrodes. To ensure good electrical contact between the sample and the electrode, fast air drying paste of silver is applied on the two sides of the sample.

## Results and discussion

### XRD studies

XRD pattern of nano CuO, HPMC/PVA blends, and HPMC/PVA-CuO (1–4%) are presented in Fig. 2. It is well reported in literature that the electrical properties of a polymer electrolyte is correlated to its crystalline nature. Higher amorphous region increases the electrical conductivity of the

polymer electrolyte sample [18, 19]. Pure CuO shows more intense and sharper peaks at around  $35.73^0$ ,  $38.78^0$  and  $48.73^0$ , whereas the characteristic broad peak of HPMC/PVA blend is shown at  $19.72^0$ . It can be seen that all the sharp peaks of nano CuO and broad peak of HPMC/PVA blends get broader

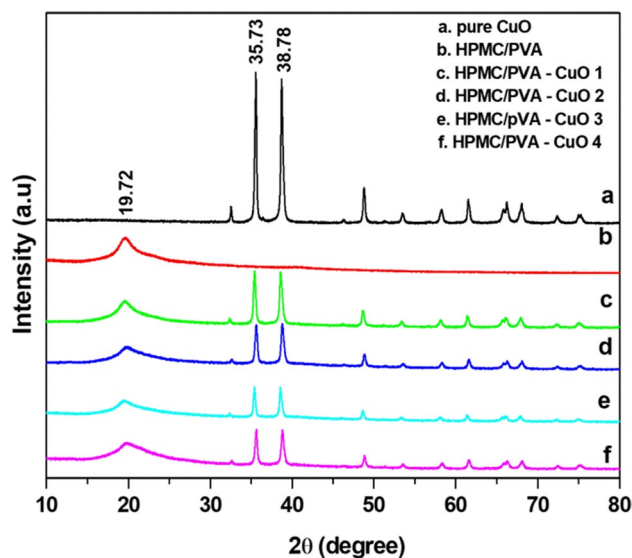


**Fig. 2** XRD pattern of pure CuO, HPMC/PVA blend, and HPMC/PVA-CuO (1–4%) polymer electrolyte films

**Table 1** Crystalline parameters for HPMC/PVA-CuO samples

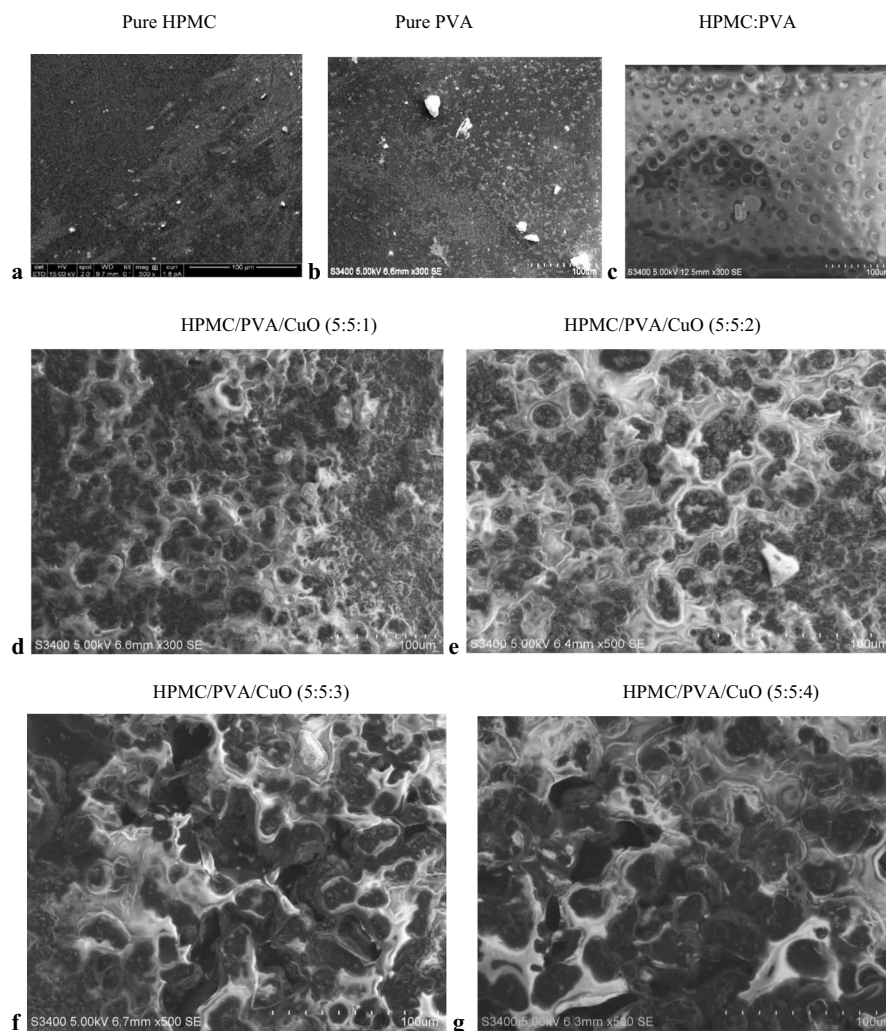
Sample	First peak				Second peak				Third peak				$X_C$ (%)
	$2\theta$ ( $^\circ$ )	d ( $\text{\AA}$ )	FWHM ( $^\circ$ )	Grain size (nm)	$2\theta$ ( $^\circ$ )	d ( $\text{\AA}$ )	FWHM ( $^\circ$ )	Grain size (nm)	$2\theta$ ( $^\circ$ )	d ( $\text{\AA}$ )	FWHM ( $^\circ$ )	Grain size (nm)	
Pure CuO	32.53	2.75	0.1943	46.4	35.56	2.52	0.1402	42.3	38.93	2.31	0.2002	43.9	57.87
HPMC/PVA blend	19.47	4.56	2.646	31.82	-	-	-	-	-	-	-	-	19.62
HPMC/PVA-CuO 1%	19.43	4.57	1.5052	55.93	35.35	2.54	0.2201	39.6	38.47	2.33	.2971	29.6	57.06
HPMC/PVA-CuO 2%	19.7	4.50	1.823	46.1	35.59	2.52	0.3166	27.52	38.79	2.32	.2606	24.8	50.03
HPMC/PVA-CuO 3%	19.48	4.55	1.6936	37.7	35.38	2.53	0.2938	29.6	38.1	2.33	.3503	24.4	31.59
HPMC/PVA-CuO 4%	19.59	4.53	2.2237	49.7	35.62	2.52	.2905	30.8	38.76	2.32	0.3543	25.1	50.32

and weaker in HPMC/PVA-CuO (1–4%) samples. The crystallite size and percentage of crystallinity are affected by the addition of CuO nanoparticles into the HPMC/PVA host polymer matrix. The percentage of crystallinity is calculated using the formula [20]:

The crystallite size is calculated using Scherrer's formula [21]:

$$L = \frac{K\lambda}{\beta\cos\theta} \quad (2)$$

$$\text{Crystallinity}(\%) = \frac{\text{Area under crystalline peaks}}{\text{Area under crystalline peaks} + \text{Area under amorphous haloes}} \times 100 \quad (1)$$

**Fig. 3** SEM photographs of HPMC/PVA-CuO polymer electrolyte films



where  $L$  is the crystallite size,  $K$  is a grain shape factor ( $K = 0.9$ ),  $\lambda$  is the wavelength of X-ray beam ( $1.5406 \text{ \AA}$ ),  $\beta$  is full width half maximum (FWHM) in radians, and  $\theta$  is the diffracted angle in radians.

The crystalline parameters tabulated in Table 1 show that the degree of crystallinity and the crystallite size decrease upon adding different ratio of CuO nanoparticles. Similar type of result was reported by Yang et al. [22], where the peak intensity of the PVA based nanocomposites greatly reduces by incorporating  $ZrO_2$  ceramic filler in the matrix. The increase in amorphous domain of the sample causes an increase in electrical conductivity of the polymer electrolytes [23].

### Morphological studies

The film morphology for pure HPMC, pure PVA, HPMC/PVA blends, and HPMC/PVA with 1–4% CuO polymer electrolyte samples are shown in Fig. 3. The conductivity properties of polymer electrolytes can be greatly influenced by the dopant CuO nanoparticles into the host polymer blend matrix of HPMC/PVA [24, 25]. Figure 3a and b show that pure HPMC and pure PVA have a surface of uniform and homogenous sort, but with various degrees of harshness. They do not show attributable crystalline region morphology, so the semi-crystallinity of HPMC and PVA is possibly to be sub-microscopic in nature [10, 26]. The SEM image of HPMC/PVA blend (Fig. 3c) exhibits uniformly distributed microporous structure. This shows that the interface similarity between the segments is one of the fundamental factors influencing the performances of polymer blends. Similar type of sheet morphology in SEM image of HPMC/PVA (50:50) blends has been reported earlier [27]. SEM images of HPMC/PVA-CuO (Fig. 3d–g) show that the complexation of CuO nanoparticles into the host polymer matrix strongly affects the morphology of HPMC/PVA blends.

The uniform spread of the CuO nanoparticles within the host polymer matrix indicates that CuO nanoparticles altogether thoroughly interacted with polymer blends [28, 29]. The different ratio of dopant CuO nanoparticles are closely packed in the polymer blend matrix, and no bare nanoparticles are seen even at the most elevated doping at 4%. This obviously shows the achievability of this strategy to configure well-distributed nanoparticles with uniform layer [30–32].

### Complex impedance spectroscopy analysis at room temperature (303 K)

#### Variation of $Z''$ with $Z'$

The complex impedance ( $Z^*$ ) as a function of the impedance modulus ( $Z'$  and  $Z''$ ) is given by the following equation [33]:

$$Z^* = Z' + iZ'' \tag{3}$$

where  $Z'$  is the real part and  $Z''$  is the imaginary part of the impedance modulus, given by

$$Z' = \frac{1}{2\pi f C_0} \left[ \frac{\epsilon''}{\epsilon'^2 + \epsilon''^2} \right], Z'' = \frac{1}{2\pi f C_0} \left[ \frac{\epsilon'}{\epsilon'^2 + \epsilon''^2} \right] \tag{4}$$

where  $f$  is frequency and  $C_0$  is the capacitance of vacuum.  $\epsilon'$  and  $\epsilon''$  are the real and imaginary parts of dielectric permittivity.

Figure 4 demonstrates the room temperature complex impedance plots of  $Z^*$  (known as Nyquist plot) for HPMC/PVA-CuO samples. A high frequency arc is seen for all samples, which is related to the bulk conduction process respectively [34, 35]. Generally, a complete, incomplete/partial, or no semicircle is observed depending on the relaxation strength and experimentally provided frequency range. The analysis of Argand plots with incomplete semicircular arc

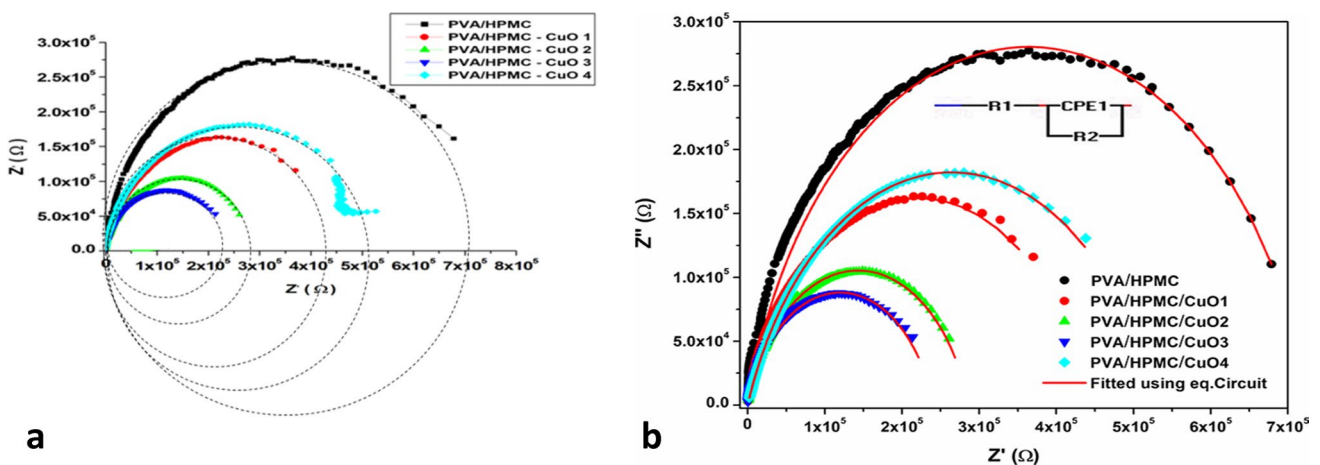


**Fig. 4** Complex impedance spectrum (Nyquist plot) for HPMC/PVA-CuO polymer electrolyte samples with electrical equivalent circuit at room temperature

**Table 2** Electrical parameters of the equivalent circuit obtained from complex impedance spectrum for HPMC/PVA-CuO concentration at room temperature

Name	$R_g$ (k $\Omega$ )	C(nF)	$n$
PVA/HPMC	727.9	0.288	0.8357
PVA/HPMC/CuO1	442.6	1.026	0.8043
PVA/HPMC/CuO2	286.2	0.576	0.8080
PVA/HPMC/CuO3	240.2	0.852	0.8056
PVA/HPMC/CuO4	529.3	0.973	0.7677

on the real impedance ( $Z'$ ) axis reveals that the charge carriers have different relaxation time [36]. The investigation of the curves from Fig. 4a shows that the semicircle displays some downturn degree rather than a half circle fixated on the genuine impedance axis. This decentralization or non-Debye sort of relaxation obeys Cole–Cole's formalism. The electrical bulk (grain) resistance ( $R_b$ ) of the polymer electrolyte sample is estimated from the intercept point of the high frequency semicircular arc with the real axis of the complex impedance. Figure 4b shows the experimental data fitted plots which is obtained by adopting an equivalent circuit formed by a resistance  $R_1$  (grain resistance  $R_g$ ) in series with a parallel combination of a constant phase element impedance ( $Z_{CPE}$ ) and resistance  $R_2$  (grain boundary resistance  $R_{gb}$ ). The equivalent configuration is of the type  $(R_1 + (R_2/Z_{CPE}))$ . The values of all fitted parameters are tabulated in Table 2. The plots clearly indicate that the  $R_b$  value decreases with increasing concentration of CuO nanoparticles and reaches to a minimum value (240 k $\Omega$ ) for HPMC/PVA-CuO (5:5:3) sample. Hence, 3 wt% CuO content nanocomposite polymer electrolyte exhibits high ionic conductivity. However, the addition of CuO nanoparticles beyond 3 wt% increased the  $R_b$  value indicating decrease in the ionic conductivity for higher dopant concentration at 4 wt%. This may be due to the accumulation of ions which

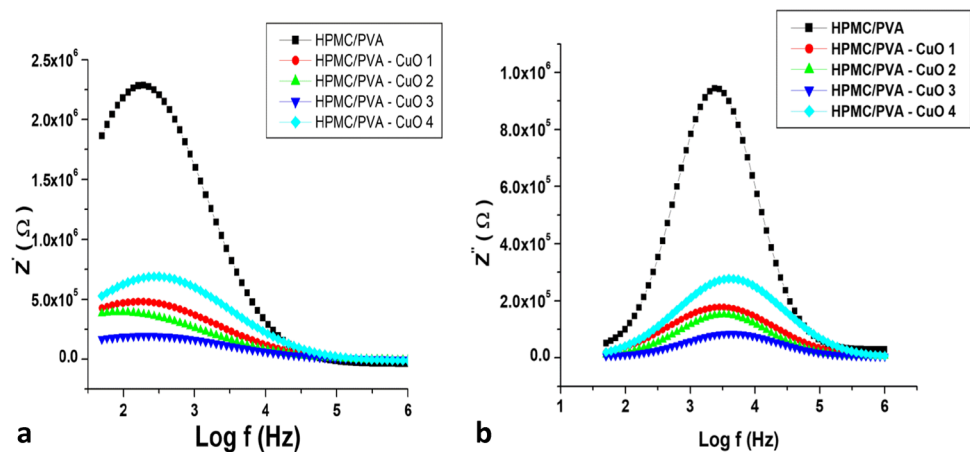
usually arises for elevated concentrations of doping, which decreases the ionic conductivity [37]. This change in ionic conductivity of polymer electrolytes is because of charge carrier density ( $n$ ) and also the mobility of charge carriers ( $\mu$ ) [38].

### Variation of $Z'$ and $Z''$ with frequency

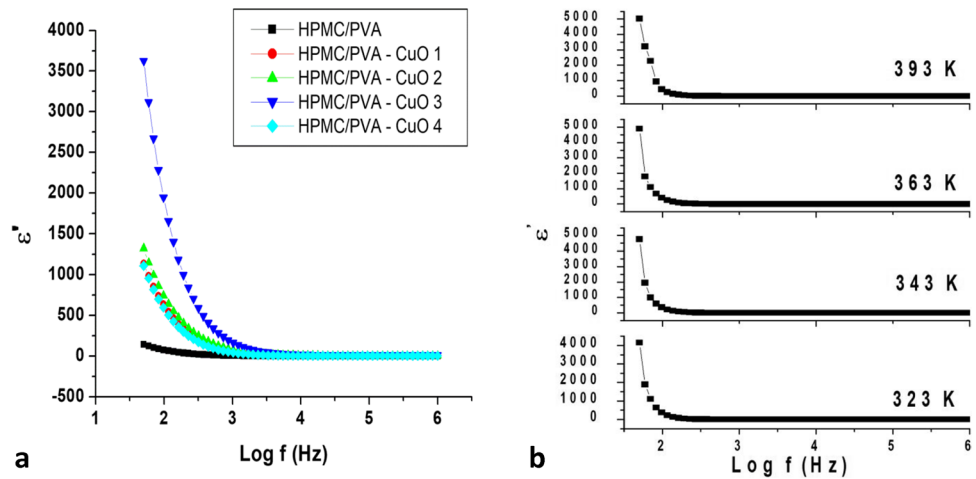
The variation of ( $Z'$ ) with Log ( $f$ ) is shown in Fig. 5a. It is observed that each sample exhibits a single broad peak for a particular frequency revealing the single relaxation process, and there after the value of  $Z'$  decreases with increasing frequency. It is observed that  $Z'$  of all samples merge completely above a certain frequency at high frequency region. This reveals the possibility in the release of space-charge polarization. As the CuO concentration increases, the maximum space charge polarization occurs at high frequency region [39, 40].

Figure 5b shows the loss spectra ( $Z''$  vs frequency) for HPMC/PVA-CuO nanocomposite polymer electrolyte samples. The appearance of broad peak in the loss spectrum confirmed the existence of relaxation behavior in these polymer electrolyte samples. The plots are more reasonable for the assessment of relaxation frequency of the most resistive component. Each sample attains a peak value of  $Z''$  at a particular frequency. It is noted that, as the CuO concentration increases, the magnitude of  $Z''$  decreases and shifts towards high frequency side. This exhibits the phenomena of electrical relaxation process in these samples. In the low frequency region, the curves seem to be dispersed, whereas they appeared to be merge for high frequency region. This behavior is because of the presence of space charge polarization in these electrolyte systems [41].

**Fig. 5** Dependence of  $Z'$  and  $Z''$  on log ( $f$ ) for HPMC/PVA-CuO electrolyte films



**Fig. 6** **a** Variation of dielectric constant as a function of log (f). **b** Variation of dielectric constant as a function of log (f) at different temperatures, for HPMC/PVA-CuO electrolyte films



**Dielectric analysis**

The design and development of electronic and electrical devices require the detail study of the parameter dielectric constant. It reveals more information on physical and chemical state of the polymer. Polymers can be designed to exhibit high dielectric constant with low dielectric loss when compared with ceramic materials [42]. Figure 6 shows the plots of dielectric constant (real part  $\epsilon'$ ) and Log (f) for varies concentrations of HPMC/PVA-CuO electrolyte systems at room temperature for frequency ranging from 50 Hz to 1 MHz. The dielectric constant  $\epsilon'$  is calculated using the relation:

$$\epsilon' = \frac{Cd}{\epsilon_0 A} \tag{5}$$

where  $C$  is the equivalent capacitance,  $d$  is the thickness of the sample,  $\epsilon_0$  is permittivity of free space, and  $A$  is the area of the sample.

Plots from Fig. 6a clearly indicate the decrease in dielectric constant as frequency increases. A significant effect of CuO nanoparticles is noticed on the dielectric constant at room temperature which leads to an increased number of

charge carriers for higher ionic conductivity and dielectric constant. The result shows that the polymer electrolyte sample of HPMC/PVA blend complexed with 3% CuO nanoparticles exhibits the high value of dielectric constant for all frequency range and indicates the highest ionic conductivity. This is also evident from AC conductivity studies (Figs. 7 and 8). But it is also noted that further increase in the CuO concentration (4 wt%) reduces the value of dielectric constant indicating that the optimum complexing of CuO nanoparticle is at 3 wt% for HPMC:PVA polymer blend. Figure 6b shows the temperature dependent dielectric constant between the temperature range (30°C – 120°C) for HPMC:PVA-CuO (5:5:3) sample. It is observed that the dielectric constant increases with increasing temperature. The high dielectric constant at low frequency is due the presence of space charge polarization at the electrode–electrolyte interface. This accumulation of charges exhibits a relaxation behavior related to that of dipolar relaxation [43]. However, the space charge accumulation at the electrode–electrolyte interface seems to be disappeared at high frequencies. This indicates that the dipoles were no longer able to follow the

**Fig. 7** **a** Variation of  $\sigma_{ac}$  as a function of log (f), **b** AC conductivity spectra at high frequency region fitted using JPL equation, for varies HPMC/PVA-CuO electrolyte films

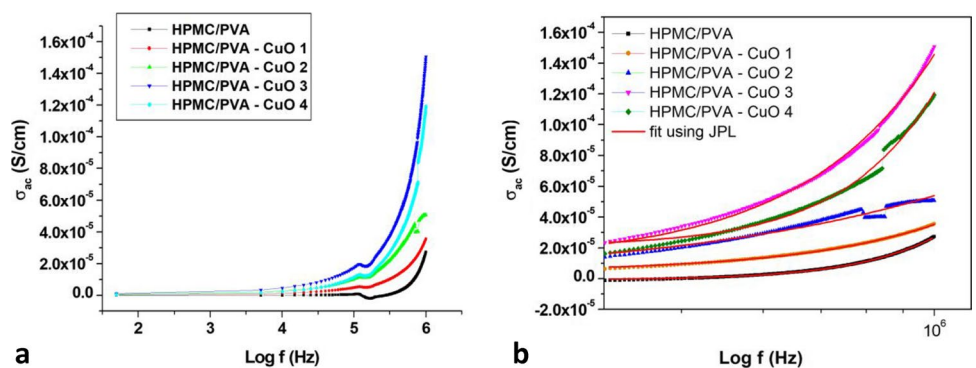


**Fig. 8** Dependence of  $\sigma_{ac}$  as a function of  $\log(f)$  for HPMC/PVA-CuO (5:5:3, wt%) sample at varies temperature

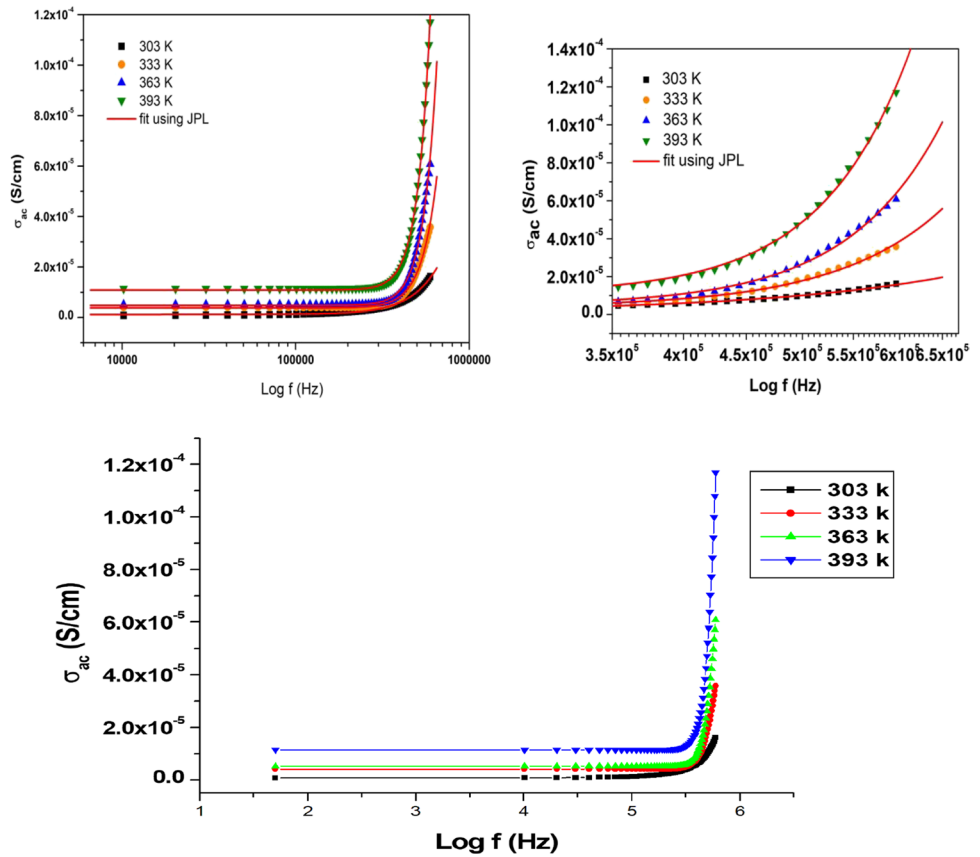


**Table 3** Comparison of parameters obtained from Jonscher Power Law fit with the experimental data of HPMC/PVA-CuO concentration at room temperature

Sample	$\sigma_{dc}$ S/cm	A	s
HPMC/PVA blends	$8.53 \times 10^{-7}$	$3.93 \times 10^{-20}$	0.78
HPMC/PVA-CuO 1%	$8.85 \times 10^{-7}$	$4.99 \times 10^{-14}$	0.56
HPMC/PVA-CuO 2%	$4.69 \times 10^{-6}$	$2.93 \times 10^{-9}$	0.71
HPMC/PVA-CuO 3%	$2.07 \times 10^{-5}$	$1.13 \times 10^{-13}$	0.51
HPMC/PVA-CuO 4%	$1.13 \times 10^{-5}$	$6.05 \times 10^{-18}$	0.68

periodic reversal of the applied electric field [44, 45]. Thus, charge carrier contribution towards polarization decreases; hence, the  $\epsilon'$  values also continuously decreases with growing frequency.

**AC conductivity analysis**

$\sigma_{ac}$  of the reported polymer-electrolyte films are calculated using real ( $Z'$ ) and imaginary ( $Z''$ ) parts of complex impedance ( $Z^*$ ) using the following equation [46]:

$$\sigma_{ac} = \left[ \frac{Z_r}{(Z_r^2 + Z_i^2)} \right] \left( \frac{t}{A} \right) \tag{6}$$

Figure 7a shows that the room temperature AC conductivity increases with frequency and attains a high value for the sample 3% HPMC/PVA-CuO. The frequency-dependent electrical conductivity for the present nanocomposite polymer-electrolyte system follows Jonscher Power Law (JPL) [47–49]. Figure 7b shows the experimental AC conductivity spectra at high frequency region fitted using JPL equation as given below:

$$\sigma(\omega) = \sigma_{dc} + A\omega^s \tag{7}$$

Here,  $\sigma(\omega)$  is the total conductivity,  $\sigma_{dc}$  is the DC conductivity of the sample,  $A\omega^s$  is the pure dispersive component of AC conductivity having a characteristic of power law in terms of angular frequency  $\omega$ , and exponent factor  $s$  ( $0 \leq s \leq 1$ ) represents the degree of interaction between mobile ions and the lattices around them. A is a constant which determines the strength of polarizability. Comparison of parameters obtained from JPL fit (Eq. 7) with the experimental data of HPMC/PVA-CuO samples at room temperature are tabulated in Table 3.



Figure 8 shows the frequency dependence of AC conductivity in 3 wt% CuO doped HPMC/PVA polymer electrolyte samples within the temperature range of 303 to 393 K. The low frequency plateau region corresponds to  $\sigma_{dc}$ . In this frequency region, the DC conductivity increases with the increasing temperature. This behavior shows that the electrical conductivity at different temperature is a thermally activated process. The inset of Fig. 8 represents JPL fitting at high frequency range for different range of temperature. It can be seen that the JPL fitting matches well with the experimental values. Conductivity at high-frequency power law region obeys  $A\omega^S$ . According to Jonscher, the origin of the frequency dependence of conductivity can be due to the relaxation phenomena of the ionic atmosphere arising from the mobile charge carriers. It is also evident from the plots that the frequency response shifts towards the high frequency dispersive region as the temperature increases. A similar type of framework in the polymer electrolyte samples of frequency-dependent

conductivity has been accounted in the literature [46, 47]. The contribution of DC conductivity at lower frequency is due to the jumping of ions from one available site to another neighboring vacant site in the host polymer matrix. This successful ion hopping takes place for the frequency lower than that of hopping frequency. The bulk conductivity of solid polymer electrolytes for all temperature signifies the frequency-independent region of the AC conductivity spectra [50]. From the figure, more dispersive conductivity is observed at higher frequencies because of the forward and backward hopping movement of ions [51].

The values of  $S$  at various temperature were determined from the slope of  $(\log\sigma)$  versus  $(\log\omega)$ . The lower value of  $S$  reflects the high conductivity of the sample. Figure 9 shows the variation of the frequency exponent ( $S$ ) as a function of temperature for 3 wt% CuO complexed HPMC/PVA polymer electrolyte sample. From the plots, it is clear that the value of  $S$  decreases with increase in temperature; hence, electrical conductivity of the sample also increases. The correlated barrier hopping (CBH) theoretical model shows that the value of  $S$  decreases with increasing temperature. Hence, CBH model is more convenient for the interpretation of conduction mechanism in these polymer electrolyte systems. CBH model gives the frequency-exponent expression as follows [52]:

$$S = 1 - \frac{6K_B T}{W_m - K_B T \ln\left(\frac{1}{\omega\tau_0}\right)} \tag{8}$$

where  $W_m$  is the maximum barrier height that ions must overcome and  $\tau_0$  is the characteristic relaxation time of the carriers. For small values,  $K_B T \ln\left(\frac{1}{\omega\tau_0}\right) \ll W_m$ . Therefore, the equation reduces to

$$S = 1 - \frac{6K_B T}{W_m} \tag{9}$$

The values of  $W_m$  can be calculated by substituting the values of  $S$  and  $T$  in Eq. 9.

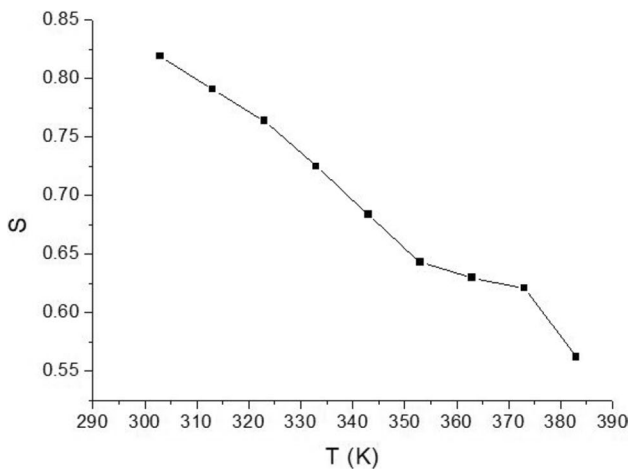
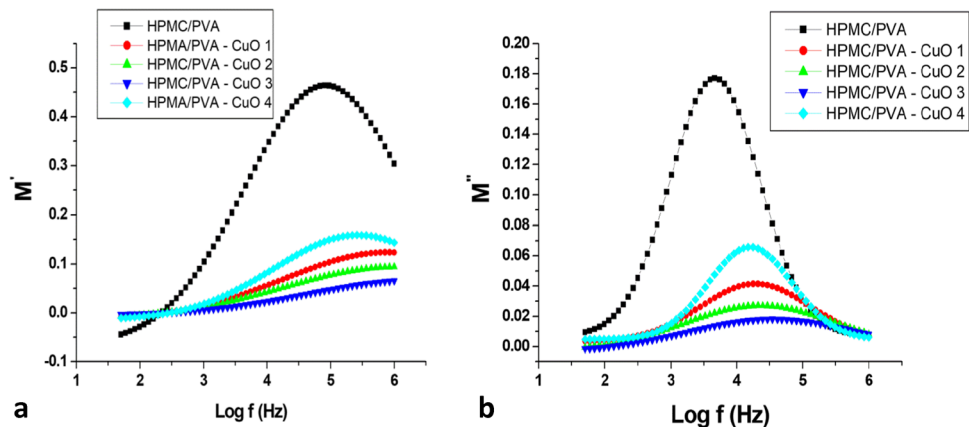
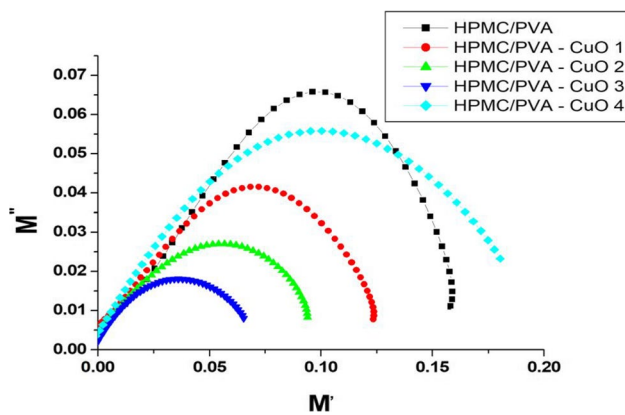


Fig. 9 Temperature effect on the frequency exponent ( $S$ ) for HPMC/PVA-CuO (5:5:3, wt%) sample

Fig. 10 **a** Dependence of  $M'$  on  $\log(f)$ . **b** Dependence of  $M''$  on  $\log(f)$  for HPMC/PVA-CuO samples





**Fig. 11** Complex electrical modulus spectrum ( $M''$  vs  $M'$ ) for different HPMC/PVA-CuO polymer electrolyte films

## Electrical modulus analysis at room temperature

### Variation of $M'$ and $M''$ with frequency

The electrical modulus analysis is convenient in understanding the relaxation behavior of ionic materials. The complex electric modulus ( $M^*$ ) can be calculated by using the following relationship [53]:

$$M^* = M' + iM'' \quad (10)$$

where

$$M' = \left[ \frac{\epsilon'}{\epsilon'^2 + \epsilon''^2} \right], M'' = \left[ \frac{\epsilon''}{\epsilon'^2 + \epsilon''^2} \right] \quad (11)$$

Figure 10a shows the dependence of the real part of the electrical modulus with  $\log(f)$  at room temperature. It is observed from the figure that, at low frequency region, the values of  $M'$  tend to be zero, confirming the absence of electrode polarization in these nanocomposites. This behavior reveals that the mechanism of conduction in these polymer electrolytes is due to the short range mobility of charge carriers.

Figure 10b shows the variation of  $M''$  with frequency at room temperature. The value of  $M''$  is nearly zero in the low frequency region and increases to a maximum value for a particular frequency and then decreases. Frequency at which,  $M''$  reaches maximum value is called as relaxation frequency. Plots from the figure clearly show that  $M''$  peaks for HPMC/PVA-CuO samples get broader and shift towards higher frequency side. This behavior confirms the dielectric relaxation in these samples. Here, the process of the hopping of charge carriers mainly dominates. The 3 wt% CuO sample exhibits a broad asymmetric peak towards higher frequency side, confirming the highest ionic conductivity. Asymmetric broadening of the peak confirms the spread of relaxation

and non-Debye type behavior in these polymer electrolyte samples [54].

### Complex electrical modulus analysis at room temperature

Figure 11 displays the room temperature spectrum of complex electrical modulus ( $M'$  vs  $M''$ ) for HPMC/PVA-CuO nanocomposite samples. The Argand plots ( $M'$  vs  $M''$ ) with an appearance of only one semicircular arc represents the presence of ionic conductivity relaxation process in these reported polymer-electrolytes [48]. Also the highest capacitance value corresponds to the smallest semicircle of the plots (HPMC/PVA-CuO 3 wt% sample). The suppression in the effect of electrode is another added advantage in the formalism of electrical modulus. Because of this reason, formalism of electrical modulus has been chosen, and the complex electrical modulus ( $M^*$ ) is calculated using Eq. 10. The plots from the Fig. 11 do not show an exact semi-circle; instead, a deformed shape of the semi-circle is seen whose centers are positioned below the  $x$ -axis. This indicates the spread of relaxation with different time constants. Therefore it can be concluded that non-Debye type of relaxation process is present in these nanocomposite polymer electrolyte systems. The non-existence of semicircular arcs with single relaxation time reveals that ion transport is associated with the segmental motion of polymer chains. Consequently, copper ion transport through HPMC/PVA blend polymer chain occurs through the viscoelastic relaxation processes [54].

## Conclusions

We have successfully synthesized copper ion conducting thin films of HPMC/PVA hosted solid nanocomposite electrolytes by adopting solution casting technique. SEM results revealed that the addition of CuO nanoparticles has a strong effect on the morphology of the polymer blends. The even distribution of CuO nanoparticles in the HPMC/PVA matrix is observed. Structural analysis by XRD suggested that both the crystallite size and the percentage of crystallinity decrease in all HPMC/PVA-CuO nanocomposites.

The analysis of dielectric constant in these samples shows that the dielectric constant value is high at low frequencies. This gives an evidence for the presence of space charge polarization. The AC conductivity spectra at high frequency region obey Jonscher Power Law. It is observed that, as the nano CuO concentration increases, the dielectric constant and ionic conductivity increases and becomes maximum for 3 w.% CuO complexed HPMC/PVA films.. The frequency exponent ( $S$ ) estimation (for HPMC/PVA-CuO 3%) at high frequency region for various temperature suggested that the correlated barrier hopping (CBH) model supports the ion transport mechanism. Hence, the sample HPMC/PVA-CuO

(3 wt%) can be suitable candidate for electrochemical cell device applications.

**Acknowledgements** Authors gratefully acknowledge the management, Vidyavardhaka College of Engineering, Mysuru, for providing financial support for this study. We thank department of Engineering Physics, VVCE, SAIF, Dharwad, for providing LCR meter and XRD facilities respectively for the reported study.

## Declarations

**Conflict of interest** The authors declare no competing interests.

## References

- Tai HL, Jiang YD, Xie GZ (2010) Preparation of surfactants directed PANI/In<sub>2</sub>O<sub>3</sub> nanocomposite thin films and its NH<sub>3</sub> sensing properties. *J Electron Sci Technol* 8(2):154–159
- Chougule MA, Patil SL, Pawar SG, Raut BT, Godse PR, Sen S, Patil VB (2012) Facile and efficient route for preparation of polypyrrole-ZnO nanocomposites: microstructural, optical and charge transport properties. *J Appl Polym Sci* 125:1418–1424
- Chougule MA, Sen S, Patil VB (2012) Polypyrrole-ZnO hybrid sensor: effect of camphor sulfonic acid doping on physical and gas sensing properties. *J Synth Mater* 162:1598–1603
- Manjunath A, Irfan M, PrasannakumarAnushree K (2016) Synthesis and characterization of CuO Nanoparticles and CuO Doped PVA Nanocomposites. *J Adv Mater Phy Chem* 7:263–273
- Naziha Suliman Alghunaim (2019) Effect of CuO nanofiller on the spectroscopic properties, dielectric permittivity and dielectric modulus of CMC/PVP nanocomposites. *J Mater Res Technol* 8(4):3596–3602
- Nigmatullin R, Lovitt R, Wright C, Linder M, Setala TN, Gama M (2004) Atomic force microscopy study of cellulose surface interaction controlled by cellulose binding domains, colloids and Surfaces. *J Bioint* 35:125–135
- Rotta J, Minatti E, Barret PLM (2011) Determination of structural and mechanical properties, diffractometry, and thermal analysis of chitosan and hydroxypropylmethylcellulose (HPMC) films plasticized with sorbitol. *J Cienc Tecnol Aliment Campinas* 31(2):450–455
- Honary S, Ebrahimi P, Emrani N (2010) The effect of plasticizer molecular weights and concentrations on water vapor permeability of hydroxypropyl methyl cellulose films. *J Pharma Bio Sci* 1(2):1–8
- Sandhya Rani N, Sannappa J, Demappa T, Mahadevaiah (2014) Structural, thermal, and electrical studies of sodium iodide (NaI)-doped hydroxypropyl methylcellulose (HPMC) polymer electrolyte films. *J Ionics* 20(2):201–207
- Sandhya Rani N, Sannappa J, Demappa T, Mahadevaiah (2015) Effects of CdCl<sub>2</sub> concentration on the structural, thermal and ionic conductivity properties of HPMC polymer electrolyte films. *J Ionics* 21:133–140
- Nouh SA, Abdel-Kader MH, Mohamed MB (2017) Structural and optical modifications in polyvinyl alcohol due to Cr<sub>2</sub>O<sub>3</sub> nanoparticles additives concentration, and gamma irradiation. *J Adv Polym Technol* 3:1–5
- Mohammed G, Morsi WM (2018) Spectroscopic, thermal and electrical properties of MgO/PVP/PVA nanocomposites. *J Phys Chem Solids* 115:238–247
- Tamgadge YS, Talwatkar SS, Sunatkari AL, Pahurkar VG, Muley GG (2015) Studies on nonlocal optical nonlinearity of Sr–CuO–polyvinyl alcohol nanocomposite thin films. *J Thin Solid Films* 595:48–55
- Sivasubramanian R, Biji P (2016) Preparation of copper (I) oxide nanohexagon decorated reduced graphene oxide nanocomposite and its application in electrochemical sensing of dopamine. *J Mater Sci Eng* 2(10):10–18
- Souza SD, Hidembergue O, Sanches EA (2018) Polyaniline–CuO hybrid nanocomposite with enhanced electrical conductivity. *J Mol Struct* 1153:20–27
- Jundale DM, Navale ST, Khuspe GD, Dalavi DS (2013) Polyaniline–CuO hybrid nanocomposites: synthesis, structural, morphological, optical and electrical transport studies. *J Mater Sci Mater Electron* 24:3526–3535
- Ali Alhazime A (2020) Effect of nano CuO doping on structural, thermal and optical properties of PVA/PEG blend. *J Inorg Organ Polym Mater* <https://doi.org/10.1007/s10904-020-01577-8>
- Ahmed HT, Abdullah O (2020) G, “Structural and ionic conductivity characterization of PEO:MC-NH<sub>4</sub>I proton-conducting polymer blend electrolytes based films.” *J. Resul. in Phy.* 16:102861
- Abdullah OG, Aziz SB, Rasheed M (2016) A Structural and optical characterization of PVA:KMnO<sub>4</sub> based solid polymer electrolyte. *J Resul in Phys* 6:1103–1108
- Ahmed HT, Abdullah OG (2019) Preparation and composition optimization of PEO:MC polymer blend films to enhance electrical conductivity. *J Polym* 11:853
- N. L. Singh, Shah S, Qureshi A, Tripathi A, Singh F, Dkavasthi, *J. Bull. Mater. Sci.*, 34: pp. 81–88 (2011).
- Yang C. C, “Study of alkaline nanocomposite polymer electrolytes based on PVA-ZrO<sub>2</sub>- KOH”, *J. Mater. Sci. Eng. B*,131:256–62, (2006).
- Azhin H. Mohamada , Omed Gh. Abdullah, Salah R. Saeed, “Effect of very fine nanoparticle and temperature on the electric and dielectric properties of MC-PbS polymer nanocomposite films”, *J. Resul. in Phys.*, 16:102898:pp 1–9, <https://doi.org/10.1016/j.rinp.2019.102898>, (2020).
- Chu PP, Reddy MJ (2003) Sm<sub>2</sub>O<sub>3</sub> composite PEO solid polymer electrolyte. *J Pow Sour* 115:288–294
- Meijje Ren H (2015) Fritz, Frimmel, Gudrun Abbt-Braun, “Multi-cycle photocatalytic degradation of bezafibrate by a cast polyvinyl alcohol/titanium dioxide (PVA/TiO<sub>2</sub>) hybrid film.” *J Molec Cataly A: Chemical* 400:42–48
- Sara Elis Bianchia (2011) Valeria Weiss Angelia, Kellen Cris-thinia Borges de Souzaa, “Evaluation of the solubility of the HPMC/PVA blends in biological fluids in vitro.” *J Mater Resea* 14(2):166–171
- Jundale D, Pawar S, Chougule M, Godse P, Patil S, Raut B (2011) Nanocrystalline CuO thin films for H<sub>2</sub>S monitoring: microstructural and optoelectronic characterization. *J Sens Technol* 1:36–46
- Jundale DM, Joshi PB, Sen S, Patil VB (2012) Nanocrystalline CuO thin films: synthesis, microstructural and optoelectronic properties. *J Mater Sci Mater Electron* 23:1492–1499
- Lee KH, Kim HY, La YM, Lee DR, Sung NH (2002) Influence of a mixing solvent with tetrahydrofuran and N, N-dimethylformamide on electrospun poly(vinyl chloride) nonwoven mats. *J Polym Sci and Polym Phys* 40:2259–2268
- Han YG, Kusunose T, Sekino T (2009) One-step reverse micelle polymerization of organic dispersible polyaniline nanoparticles. *J Synth Mater* 159:123–131
- Jundale DM, Navale ST, Khuspe GD, Dalavi DS, Patil PS, Patil VB (2013) Polyaniline–CuO hybrid nanocomposites: synthesis, structural, morphological, optical and electrical transport studies. *J Mater Sci: Mater Electron* 24:3526–3535

32. Sahoo S, Hajra S, Mohantha K, Choudhary RNP (2018) Processing dielectric and impedance spectroscopy of lead free BaTiO<sub>3</sub>, BiFeO<sub>3</sub> CaSnO<sub>3</sub>. *J Alloy Comp* 766:25–32
33. Jonscher AK (2000) Dielectric Relaxation in low loss Solids. *J molec liqu* 86(1–3):259–268
34. Aziz SB, Abdullah RM, Rasheed MA, Ahmed HM (2017) Role of ion dissociation on DC conductivity and silver nanoparticle formation in PVA: AgNt based polymer electrolytes: Deep insights to ion transport mechanism. *J Polym* 9(8):338
35. Aziz SB (2015) Study of electrical percolation phenomenon from the dielectric and electric modulus analysis. *J Bull Mater Sci* 38:1597–1602
36. S. B. Aziz, Omed Gh. Abdullah, R. Salah, Saeed, Hameed M. Ahmed, “Electrical and dielectric properties of copper ion conducting solid polymer electrolytes based on chitosan: CBH model for ion transport mechanism”, *Int. J. Electrochem. Sci.* 13:3812 – 3826 (2018).
37. Abdullah OG, Saleem SA (2016) Effect of Copper sulfide nanoparticles on the optical and electrical behavior of poly(vinyl alcohol) films. *J Elec Mater* 45:5910–5920
38. Aziz SB (2013) Li<sup>+</sup> ion conduction mechanism in poly( $\epsilon$ -caprolactone)-based electrolyte. *Iran Polym J* 22:877–883
39. R. Baskaran, Selvasekarapandian, G. Hiran kumar, M. S. Bhuvaneshwari, “Dielectric and conductivity relaxations in PVAc based polymer electrolytes”, *J. Ionics.* 10:29–34 (2004).
40. Abd El-Kader, F. H. Osman, K. H. Mahmoud, M. A. F. Basha, “Dielectric investigations and AC conductivity of polyvinyl alcohol films doped with europium and terbium chloride”, *J. Phys. B: Condens. Matt.*, 20084 03:3473–3484 (2008).
41. Mudarra M, Calleja RD, Belana J, Canadas JC, Diego JA, Sellares J (2001) Study of space charge relaxation in PMMA at high temperatures by dynamic electrical analysis. *J Polym* 42(4):1647–1651
42. Ibrahim S, Yasin SMM, Nee NM, Ahmad R, Johan MR (2012) Conductivity and dielectric behavior of PEO-based solid nanocomposite polymer electrolyte. *J Soli Sta Commun* 152(5):426–434
43. Aziz SB, Abidin ZHZ (2014) Electrical and morphological analysis of chitosan:AgTf solid electrolyte. *J Mater Chem Phys* 144:280–286
44. Aziz SB (2016) Occurrence of electrical percolation threshold and observation of phase transition in chitosan<sub>(1-x)</sub>:AgI<sub>x</sub> (0.05 ≤ x ≤ 0.2) based ion conducting solid polymer composites. *J Appl Phys* 122:706
45. Aziz SB, Abidin ZHZ (2015) Ion-transport study in nanocomposite solid polymer electrolytes based on chitosan: electrical and dielectric analysis. *J Appl Polym Sci* 132:41774
46. Gurbuz O, Senkal BF, Icelli O (2017) Structural, optical and electrical properties of polypyrrole in an ionic liquid. *J Polym Bull* 74:2625–2639
47. Jonscher AK (1977) The Universal dielectric response. *J Nature* 267:673–679
48. Ramesh S, Liew CW (2012) Exploration on nano-composite fumed silica-based composite polymer electrolytes with doping of ionic liquid. *J Non-Cryst Soli* 358:931–940
49. Funke K (1993) Jump relaxation in solid electrolytes. *J Prog Solid State Chem* 22:111–195
50. Z. Imran, M. A. Rafiq, M. Ahmad, K. Rasool, S. S. Batool, M. M. Hasan, “Temperature dependent transport and dielectric properties of cadmium titanate nanofiber mats”, *J. AIP Advances*, 3:032146 (2013).
51. Maji P, Pande PP, Choudary RB (2015) Effect of Zn(NO<sub>3</sub>)<sub>2</sub> filler on the dielectric permittivity and electrical modulus of PMMA. *J Bull Mater Sci* 38:17–24
52. Mohamed K, Gerasimov TG, Moussy F, Harmon JP (2005) A broad spectrum analysis of the dielectric properties of poly(2-hydroxyethyl methacrylate). *J Polymer* 46:3847–3855
53. Ranjan R, Kumar R, Kumar N, Behera B, Choudhary RNP (2011) Impedance and electric modulus analysis of Sm-modified Pb(Zr<sub>0.55</sub>Ti<sub>0.45</sub>)<sub>1-x/4</sub>O<sub>3</sub> ceramics. *J Alloy Compd* 509:6388–6394
54. Aziz SB, Rasheed MA, Abidin ZHZ (2017) Optical and electrical characteristics of silver ion conducting nanocomposites solid polymer electrolytes based on chitosan. *J Electron Mater* 46:6119–6130

**Publisher's note** Springer Nature remains neutral with regard to jurisdictional claims in published maps and institutional affiliations.